A HYBRID APPROACH TO MODEL AND SIMULATE THE DOUBLE-GIMBALED MEMS-BASED MICROMIRROR

Ivan Plander[1], Michal Stepanovsky[1,2]

[1]A.Dubcek University of Trencin
911 50 Trencin, Studentska 2, Slovakia

[2]Czech Technical University in Prague
166 36 Praha 6, Zikova 4, Czech Republic

plander@tnuni.sk (Ivan Plander)

Abstract

In this paper, the hybrid approach to model and simulate the behavior of the double-gimbaled MEMS-based micrommiror is presented. The model of the micromirror is represented as a system of coupled equations and combines both the distributed and lumped parameter description. The advantage of the hybrid approach is improved accuracy of simulation results in comparison with the results obtained from pure lumped parameter models, and on other hand, the enormous reduction in simulation time in comparison with the models completely based on the distributed parameter description. The model involves electrostatics, solid mechanics and gas dynamics. Thus, the multiphysics interactions have to be considered and therefore they are discussed in the paper. The gas-damping is modeled by the finite element analysis (via squeeze-film damping effect), and thus, there is no need for the derivation of the analytical formula of the gas-damping.

Keywords: Hybrid model, Multiphysics interactions, MEMS-based micromirror, FEM

Presenting Author's biography

Michal Stepanovsky received the MSc and PhD degrees in mechatronics from the Alexander Dubcek University of Trencin. His research interests include the design of optical switches for all-optical networks and multi-physics simulation of dynamical systems by using finite element analysis, especially the simulation of the MEMS-based devices. He is interested in the modeling and simulation of the mechatronic systems and also in the parallel computer architectures.

1 Introduction

The micro-electro-mechanical system (MEMS) technology, especially the MEMS-based micromirrors, has great practice (more than 20 years) in all-optical comunication networks research. The designed micromirrors, as a class of significant MEMS-based actuators, found utilization in various modern micro-opto-electro-mechanical systems (MOEMS), such as scanners [1, 2], projection displays [3, 4], and optical switches for all-optical networks [5–9]. The application of MEMS for large-scale all-optical networks is still the only solution until optical transistors will be available.

The double-gimbaled electrostatically actuated micromirror is nonlinear multiphysics device [10]. The model of the micromirror is useful tool for its design and optimization. It allows to optimize the shape and dimensions of the micromirror and their suspension. Moreover, this model can be simply complemented with a model of control circuits and thus it is possible to simulate the micromirror response for different control strategies. A schematic view on the micromirror is shown in Fig. 1. The mirror plate is suspended by a double-gimballed structure, which consists of two pairs of torsional hinges (springs) and a micromirror frame. The micromirror can be tilted about two axes by electrostatic actuation using four control voltages applied to the electrodes underneath the mirror, and translated along z-axis.

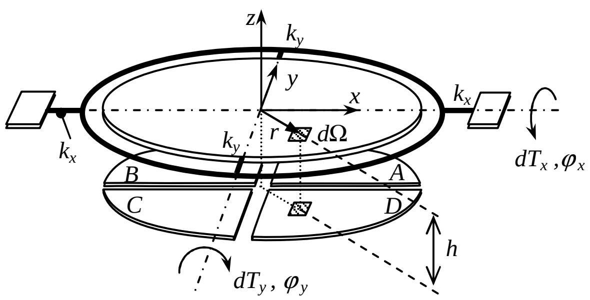

Fig. 1 Schematic view of the micromirror

The most of current literature typically consider the lumped parameter models [11-18]. The drawback of this approach is coarse approximation of actual behavior of the micromirror. On the other hand, the pure distributed parameter model approach is highly time consuming and unpractical to solve by personal computers. Thus, the combination of both of them can take the advantage.

2 Multiphysics model

The multiphysics model can be divided into three parts according to occurring physical phenomena and interactions between them as shown in Fig. 2. If a voltage is applied, created electrostatic field affects mechanical structure through electrostatic forces and the micromirror is attracted to the electrodes. This makes new geometry configuration and different electric field distribution. Moreover, geometry change, i.e. as the micromirror is moving, it generates a motion of surrounding gas, which induces surface forces (pressure) affecting motion of the micromirror. Because the micromirror is not perfectly rigid planar plate, the output from the model is continuous both in space and time.

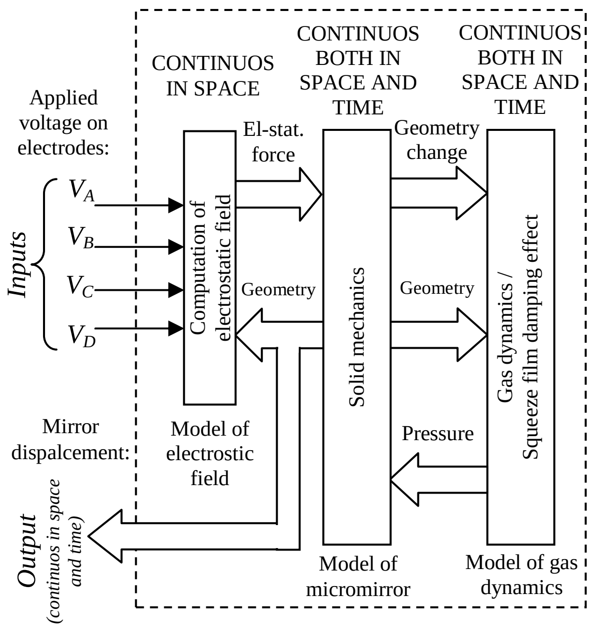

Fig. 2 Multiphysics model

First of all, the governing equations for all three physical phenomena have to be specified. This step determines the accuracy of the model. In general, an electrostatics part of the model is described by the Poisson equation, a mechanics part is described by the Newton equations, and a fluid dynamics part is decscribed by the Navier-Stokes equations. This description produces the model with distributed parameters as it is shown in Fig.2.

To simulate processes in the model by a computer system, both the time and spatial discretization have to be applied to obtain difference equations and consequently the system of algebraic equations. The model as shown in Fig.2 is continuous in time and in space. The spatial dicretization by standard Galerkin finite element method (standard GFEM) can be used for electrostatics and solid mechanics; and then the Newmark method for time stepping can be used only for solid mechanics. The temporal discretization by characteristic-Galerkin procedure and after that the standard GFEM for spatial discretization would be used for gas dynamics because of convection-dominated problem. This results in finite number of unknown values of searched quantity (gas pressure, electric field intensity) corresponding to certain points (nodes) of the spatial domain, the so-called discretization points. Thus, the matrix equations will be obtained and they can be subsequently solved.

As shown in [19] the simulation time in system with 100 GFLOPS of performance varies in range from one day to one hundred days for only 10^6 to 10^8 of finite element mesh nodes considering the Poisson, Newton and full Navier-Stokes differential equations. The precision of simulation results is highly depending on the total number of discretization nodes. It is evident that without simplifications the model based on the pure distributed parameter description can be simulated only by the high-performance parallel computer system.

2.1 Hybrid multiphysics model

Frequently, two or more different physical systems interact with each other, with independent solution of any one system being unfeasible without concurrent solution of the others. Such systems are known as coupled, and of course, this is the case of the electrostatically actuated gas-damped double-gimbaled micromirror. The coupling occurs on the domain interfaces via the boundary conditions imposed there, and it is applied into the corresponding finite element mesh nodes during the simulation process. In the simplest case, the finite element mesh nodes are mapped one-to-one on the physical boundary as shows Fig. 3. As one can see, the interacting physical domains have shared the nodes on the boundary, and thus, the computation of coupling is straightforward and it is determined by coupling equations.

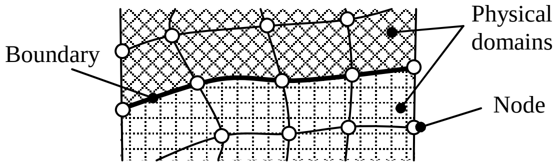

Fig. 3 Coupling via boundaries

In the hybrid models, in which one or more physical domains are omitted and replaced by the lumped parameter description, it arises the necessity of the additional computation between their partial models. To consider interactions from lumped parameter model to distributed parameter model on one hand, and from distributed parameter model to lumped parameter model on the other hand, the expansion/reduction to distributed/lumped parameter description have to be involved into the hybrid model.

In our hybrid model of the micromirror we suppose that the micromirror plate and outer frame are rigid, the deformation of the torsional hinges is linearly proportional to the stress applied to them, and the material damping in the hinges can be neglected. Therefore, the mechanical properties of the micromirror and their suspensions can be approximated by only six parameters – mass, moments of inertial about axes of rotation and spring constants. Moreover, the pressure distribution over the micromirror surface can be modeled by the squeeze film damping effect. The motion of the viscous fluid is described by the Navier-Stokes equations. Nevertheless, the nonlinear behavior of the squeeze film damping is typically approximated by the Reynolds equation [20–22] because of simplicity. These simplifications results in the hybrid multiphysics model as shown in Fig. 4.

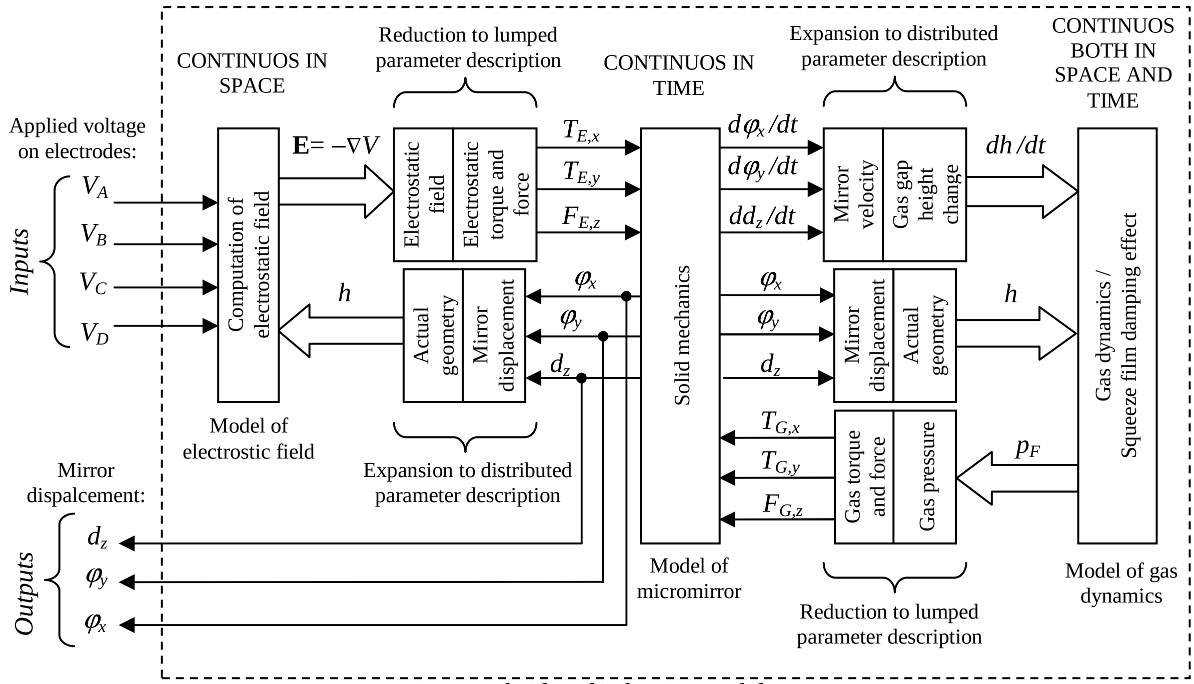

Fig. 4 Hybrid multiphysics model

2.2 Governing equations of the hybrid model

The differential equation of the micromirror motion is given as follows

$$\mathbf{J}\ddot{\boldsymbol{\zeta}}+\mathbf{K}\boldsymbol{\zeta}+\boldsymbol{\Psi}_G=\boldsymbol{\Psi}_E, \qquad (1)$$

where **J** and **K** are mass and spring matrices, respectively. The components of $\boldsymbol{\Psi}_G$ include the torques and force developed by the gas; and the components of the $\boldsymbol{\Psi}_E$ include electrostatic actuation torques and force, respectively. The both terms $\boldsymbol{\Psi}_G$ and $\boldsymbol{\Psi}_E$ are complex functions of the vector $\boldsymbol{\zeta}$. The vector $\boldsymbol{\zeta}$ represents the angular and vertical displacement of the micromirror. The Newton's notation is used to represent the time derivation. The symbols **J**, **K**, $\boldsymbol{\Psi}_G$, $\boldsymbol{\Psi}_E$ and $\boldsymbol{\zeta}$ are defined as follows

$$\mathbf{J}=\begin{pmatrix} I_x & 0 & 0\\ 0 & I_y & 0\\ 0 & 0 & m\end{pmatrix},\ \mathbf{K}=\begin{pmatrix} K_x & 0 & 0\\ 0 & K_y & 0\\ 0 & 0 & K_z\end{pmatrix}, \qquad (2)$$

$$\boldsymbol{\Psi}_G=\begin{pmatrix} T_{G,x}\\ T_{G,y}\\ F_{G,z}\end{pmatrix},\ \boldsymbol{\Psi}_E=\begin{pmatrix} T_{E,x}\\ T_{E,y}\\ F_{E,z}\end{pmatrix},\ \boldsymbol{\zeta}=\begin{pmatrix} \varphi_x\\ \varphi_y\\ d_z\end{pmatrix},$$

where I_x and I_y are moments of inertia about x and y axis; m is the mass; K_x and K_y are torsion spring constants for rotation about x and y axis; K_z is the bending spring constant in z axis; $T_{G,x}$ and $T_{G,y}$ are x and y components of gas torque; $F_{G,z}$ is gas force in z axis; $T_{E,x}$ and $T_{E,y}$ are x and y components of electrostatic driving torque; $F_{E,z}$ is electrostatic driving force in z axis; φ_x, and φ_y are x and y components of angular displacement of the micromirror; d_z is vertical displacement of the micromirror. The constants I_x, I_y, m, K_x, K_y and K_z can be determined easily (analytically, numerically or experimentally), thus they are out of our interest.

The components of the gas vector $\boldsymbol{\Psi}_G=(T_{G,x}\ \ T_{G,y}\ \ F_{G,z})^{\mathrm{T}}$ are given as follows

$$T_{G,x}=\int_{\Omega_{m+f}} y\,p_F\,d\Omega,$$

$$T_{G,y}=\int_{\Omega_m} x\,p_F\,d\Omega, \qquad (4)$$

$$F_{G,z}=\int_{\Omega_{m+f}} p_F\,d\Omega,$$

where Ω_m is the area of the micromirror bottom surface (micromirror side closer to the electrodes), $\Omega_{m+f}=\Omega_m\cup\Omega_f$, where Ω_f is the area of micromirror frame bottom surface; and p_F is perturbation pressure in the point $(x, y)\in\Omega_{m+f}$, which affects on the element of surface $d\Omega$. We use the symbol Ω in later equations instead of Ω_{m+f} for the clarity.

The perturbation pressure p_F can be approximated by linerized Reynolds equation in the form

$$\frac{p_A h^2 Q_{ch}}{12\mu}\nabla^2 p_F-\frac{dp_F}{dt}-\frac{p_A}{h}\frac{dh}{dt}=0, \qquad (5)$$

where p_A is the ambient pressure, h is the actual gas gap height (distance between surface element dS and the electrodes), μ denotes the fluid viscosity at normal conditions. The term Q_{ch} is the relative flow rate function that accounts for the rarefied gas effects. According to model proposed in [19]:

$$Q_{ch}=1+0{,}07744K_{Kn}+6{,}30361K_{Kn}^{\,1{,}17468}, \qquad (6)$$

where K_{Kn} is Knudsen number defined as the ratio of the molecular mean free path to a representative physical length scale, and h is given as follows

$$h=h_0-x\sin(\varphi_y)-y\sin(\varphi_x)\cos(\varphi_y)-d_z \qquad (7)$$

for $x, y\in\Omega_m$,

or

$$h=h_0-y\sin(\varphi_x)-d_z \qquad (8)$$

for $x, y\in\Omega_f$.

The equation (5) is used for gas damping estimation; the real damping may be different.

The components of the vector $\boldsymbol{\Psi}_E=(T_{E,x}\ \ T_{E,y}\ \ F_{E,z})^{\mathrm{T}}$ are given as follows

$$T_{E,x}=\int_{\Omega_z} y\,p_E\,d\Omega=\frac{\varepsilon}{2}\sum_{i=A,B,C,D}\ \int_{\Omega_{m,i}}\frac{yV_i^2}{h^2}d\Omega,$$

$$T_{E,y}=\int_{\Omega_z} x\,p_E\,d\Omega=\frac{\varepsilon}{2}\sum_{i=A,B,C,D}\ \int_{\Omega_{m,i}}\frac{xV_i^2}{h^2}d\Omega, \qquad (9)$$

$$F_{E,z}=\int_{\Omega_z} p_E\,d\Omega=\frac{\varepsilon}{2}\sum_{i=A,B,C,D}\ \int_{\Omega_{m,i}}\frac{V_i^2}{h^2}d\Omega,$$

where p_E is electrostatic pressure, ε is the permitivity of the free space, $\Omega_{m,i}$ and V_i (for $i = A, B, C$ and D) are the micromirror surfaces over the electrodes marked by symbol i (see Fig.1) and the voltages applied to them, respectively.

In equations (9) we suppose that the electric field intensity E can be computed as ratio of V_i / h, what means that the electrostatic field rarefaction effects are neglected. Thus, the equation

$$E=\frac{V}{h}, \qquad (10)$$

is used to approximate electric field intensity over the micormirror surface.

Regardless the used simplifications in the electrostatics and gas dynamics, the model of electrostatics and gas dynamics still remain described by distributed parameters. Only solid mechanics part of the model is described by the lumped parameters. The equations (1), (5) and (10) model the solid mechanic, gas dynamic and electrostatic part of the hybrid model; and the equations (4), (7-8) and (9) are used for the expansion/reduction to distributed/lumped parameter description.

The micromirror behavior is nonlinear in nature. The two-way coupling between electrostatic field and micromirror structure is the dominant phenomena creating the nonlinearity of the system, regardless the fact that the solid mechanics is modeled by the linear Hook's law and the electrostatic field is determined by the Poisson equation, which is also linear. Moreover, the angular displacements about x and y axis are not independent, they are closely related on each other.

Even in the static case, when the time derivation and the gas term $\mathbf{\Psi}_G$ disappear from the equation (1), the nonlinear behavior can be observed. In this case, the equation (1) is reduced to

$$\mathbf{K}\zeta = \mathbf{\Psi}_E, \tag{11}$$

what means, that the static equilibrium is satisfied.

3 Simulation results

In contrast to pure distributed parameter model based on the Poisson, Newton and full Navier-Stokes differential equations, the simulation time of the hybrid model (presented in section 2.2) less than few minutes can be achieved at the personal computer with 10 GFLOPS of performance.

In our case, the micromirror surface was discretized by the 4700 linear triangular elements with about 2500 of mesh nodes. Thus, the searched quantities (perturbation pressure p_F and electric field intensity E) were evaluated only in the 2500 of spatial nodes over the micromirror surface. This discretization is sufficiently fine because the micromirror surface is planar structure and thus there is no need for the expansion into the third dimension. The simulation of the response of the micromirror during 20 ms with simulation step time of 10 µs takes about 2 hours at the computer with 4 GFLOPS. The simulation results are discussed in the next sections.

3.1 Non-optimized micromirror

We have simulated the micromirror as shown in Fig. 5 with parameters as given in the Tab.1.

Micromirror diameter	D_1	600 µm
Micromirror thickness	---	4 µm
Frame inner diameter	D_2	626 µm
Frame outer diameter	D_3	668 µm
Frame thickness	---	4 µm
Suspension beam length	L	74 µm
Suspension beam width	w	3 µm
Suspension beam thickness	---	1 µm
Micromirror–substrate distance	---	130 µm

Tab. 1 Dimensions of the simulated micromirror

The micromirror material was considered to be isotropic, with the fracture strength 7 GPa, Young's modulus of 169 GPa, Poisson ratio of 0.22, and density of 2330 kgm^{-3}. The mean free path of the molecules of the gas is supposed to be equal to 0.25 µm, ambient gas pressure 1.01225 kPa, gas viscosity 20.10^{-6} m^{2}s^{-1}, and ambient temperature 294.15 K.

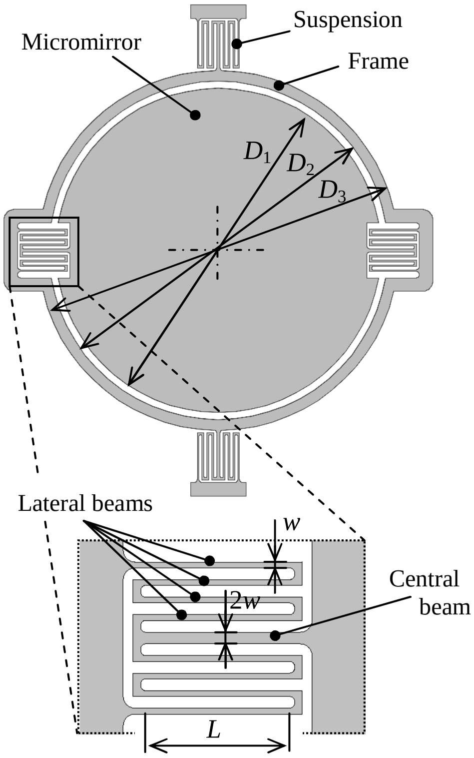

Fig. 5 Micromirror with detailed view on the suspension

The position of the micromirror is determined by the voltages applied to electrodes underneath the micromirror. The Fig. 6 shows the step response of the mirror when U_A = 90 V and U_B = U_C = U_D = 0 V. In the figure, the components of ζ vector are shown.

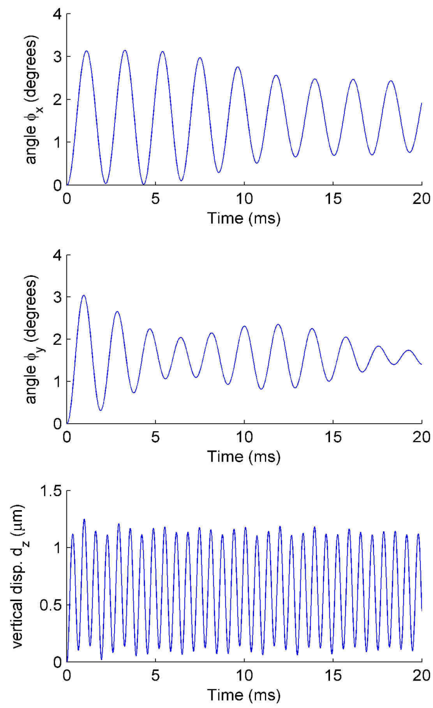

Fig. 6 Step response of the micormirror

The time-avoided angle-angle diagram of micromirror motion is shown in Fig. 7. As one can see, the micromirror starts in (0; 0) point and oscilates around its stable point of (1.578; 1.578). The micromirror is tilting about two axes. The motion is not matched, and thus, the deviation from ideal trajectory (the straight line from the starting point to the target) occurs. This behavior is unsuitable and it is result of cross-axis coupling and non-optimal micromirror design.

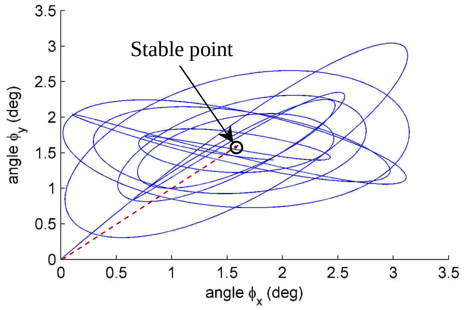

Fig. 7 Angle-angle diagram

The energy disipation during micromirror motion can be observed from the angle-velocity diagrams for both *x* and *y* axis, as it is shown in Fig. 8. The expected spiral trajectory is deformed due to dominant cross-axis coupling effect.

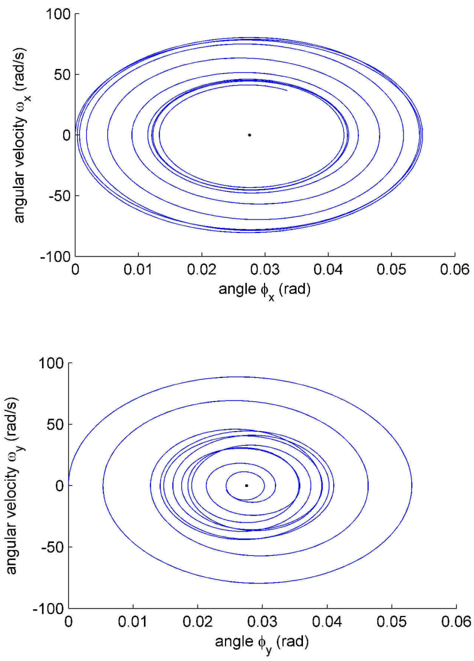

Fig. 8 Angle-velocity diagrams

3.2 Optimized micromirror

As shown in the previous section, the non-optimized micromirror motion is strongly affected by cross-axis coupling. However, if the dimensions of the micormirror and its suspensions are optimized, the effect of the cross-axis coupling can be eliminated. Neverheless, the cross-axis coupling still exists and have to be considered. The step response of the optimized micromirror for the same actuating voltage as in the section 3.1 is shown in the Fig. 9. The figure shows the components of ζ vector**.**

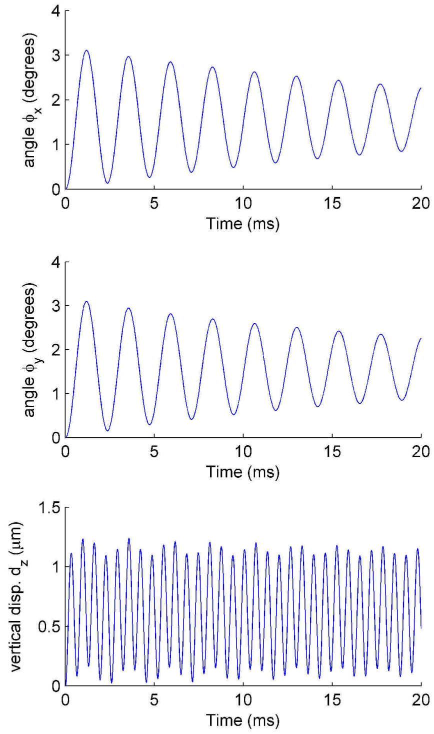

Fig. 9 Step response of the micormirror

The time-avoided angle-angle diagram of micromirror motion is shown in Fig. 10. As one can see by comparing Fig. 7 and Fig. 10, after the optimization, the improved behavior is achieved.

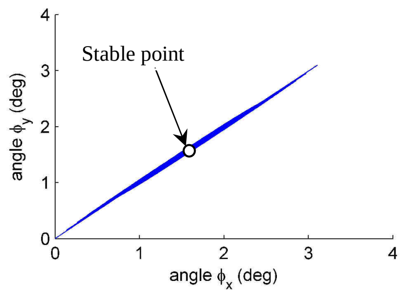

Fig. 10 Angle-angle diagram

The micromirror is moving along the ideal trajectory. This indicates better dynamic characteristics and better controllability of micromirror motion. The application of the micromirror in the all-optical switches requires the short swithing time as much as possible, i.e. the micromirror have to adopt new steady-state position in minimal time. Until the mechanical structure is not optimized, the used control strategy would take account of non-optimal micromirror design. Therefore, the optimization of the micromirror structure is very important step in its design regardless the control strategy. The angle-velocity diagrams of optimized micromirror for both *x* and *y* axis are shown in Fig. 11.

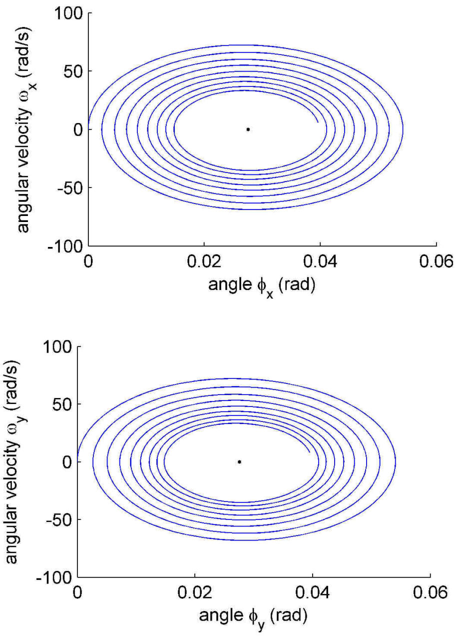

Fig. 11 Angle-velocity diagrams

4 Conclusion

The multiphysics approach represent significant tool to model and simulate various systems. It makes it possible to model and simulate the most important parts of the system in detail, and simplify the unsubstantial ones. The crucial parts of the system can be modeled by distributed parameters, while the others by the lumped parameters. It allows to balance between computational complexity (and/or computational time) and precisions of simulation results. Moreover, the simulation results can be used for the advanced design of parameters of the system. Thus, the optimization can be realized before fabrication. It is not possible to optimize the micromirror parameters without adequate model reflecting all physical phenomena at appropriate level of simplification. Presented hybrid model is a model with both distributed and lumped parameters, and is suitable for designers of MEMS-based all-optical switches. Improved controllability of the optimized micromirror makes it possible to obtain the switching time less than 2 ms in open-loop control when the suitable shape of the applied control voltage is used.

References

[1] Papageorgas P.G. – Maroulis D. – Anagnostopoulos G. et al.: A High-Performance Imaging and Control System for a Micromirror-Based Laser-Scanning Endoscope Device. IEEE Transactions on instrumentation and measurement, Vol. 55, No. 5, Oct. 2006, pp. 1725 – 1733.

[2] YEOW, J. T. W. – YANG V. X. D. et al.: *Micromachined 2-D scanner for 3-D optical coherence tomography.* Sensors and Actuators A: Physical, Vol. 117, Issue 2, 14 Jan. 2005, pp.331-340.

[3] Van Kessel, P.F. Hornbeck, L.J. Meier, R.E. Douglass, M.R.: A MEMS-based projection display. Proc. of the IEEE. Vol. 86, Issue 8, Aug 1998, pp. 1687-1704.

[4] Kerwin Wang et al.: Micro-optical Components for a MEMS Integrated Display. In: *The 12th Int. Workshop on The Physics of Semiconductor Devices (IWPSD)*, Chennai, India, December 16-20, 2003.

[5] MASAAKI KAWAI – KAZUYUKI MORI – TSUYOSHI YAMAMOTO et al.*: Optical Components and Devices for Next-Generation Photonic Networks*. Fujitsu Sci. Tech. Journal, 42, 4, October 2006, p.483–493.

[6] KAMAN, V. – HELKEY, R.J. – BOWERS, J.E.: *Compact and Scalable Three-Dimensional Microelectromechanical System Optical Switches*. In: Journal of Optical Networking, Vol.6, No.1, January 2007, pp.19-24.

[7] WU, M. C. – SOLGAARD, O. – FORD, J. E.: *Optical MEMS for Lightwave Communication. Journal of Lightwave Technology*, Vol.24, No.12, Dec.2006. pp. 4433-4454.

[8] XUEZHE ZHENG – VOLKAN KAMAN et al.: *Three-Dimensional MEMS Photonic Cross-Connect Switch Design and Performance*. IEEE J. of Selected Topics in Quantum Electronics, Vol.9, No.2, March/April 2003. pp.571-578.

[9] Plander I: Nonblocking All-Optical Multicast Three-Stage Clos Networks. In: Proc. Of the Int. Conf. on Computing, Communications and Control Technologies. Texas (USA), Austin, Aug. 14-17, 2004. Vol VII, pp.215-220.

[10] Plander, I. – Stepanovsky, M.: Modeling and Simulation of Gas-Damped Electrostatic Actuators of MEMS Devices. In: Proc. of the 13th World Multi-Conference on Systemics, Cybernetics and Informatics; July 10–13, 2009; Orlando, Florida, USA. Vol 3, pp.251 - 256.

[11] ZHIXIONG XIAO; WUYONG PENG ; XINGTAO WU ; FARMER K. R. : Pull-in study for round double-gimbaled electrostatic torsion actuators. Journal of micromechanics and microengineering, 2002, vol. 12, n.1, pp. 77-81.

[12] ZHANG X. M. ; CHAU F. S. ; QUAN C. ; LAM Y. L.; LIU A. Q.; A study of the static characteristics of a torsional micromirror, Sensors and actuators. A, Physical, 2001, vol. 90, n.1-2, pp. 73-81.

[13] Jian Ping Zhaoa et al: A study of dynamic characteristics and simulation of MEMS torsional micromirrors. Sensors and Actuators A: Physical. Vol. 120, Issue 1, 29 April 2005, pp. 199-210.

[14] Y. Zhao, F. E. H. Tay, G. Zhou, F. S. Chau, A study of electrostatic spring softening for dual-axis micromirror, Optik 117 (2006), pp. 367–372.

[15] Y. Yao, X. Zhang, G. Wang, L. Huang, Efficient modeling of a biaxial micromirror with decoupled mechanism, Sensors and Actuators A 120 (2005), pp. 7–16.

[16] Jin-Chern Chiou and Yu-Chen Lin, A Multiple Electrostatic Electrodes Torsion Micromirror Device With Linear Stepping Angle Effect, Journ. of microelectomechanical systems, Vol.12, No.6, Dec. 2003, pp.913-920.

[17] YAMAMOTO, T. – YAMAGUCHI, J. et al.: *Development of a Large-scale 3D MEMS Optical Switch Module*. NTT Tech. Review. Vol.1, No.7., Oct. 2003. pp. 37-42.

[18] Zhou, G. et al.: Neural Network Approach for Linearization of the Electrostatically Actuated Double-Gimballed Micromirror. Springer: Analog Integrated Circuits and Signal Processing. Vol. 40, No.2, Aug. 2004, pp. 141–153.

[19] Plander, I. - Stepanovsky, M.: The distributed parameter Model of the Electrostatic-Actuated Gas-Damped MEMS-based Devices for the Simulation on the Parallel Computer Systems. In: 5th Int. Workshop on Grid Computing for Complex Problems - GCCP 2009. Oct. 2009, Bratislava.

[20] PAN, F. – KUBBY, J. – PEETERS, E. et al.: Squeeze film damping effect on the dynamic response of a MEMS torsion mirror. Tech. Proc. of the 1998 Int. Conf. on Modeling and Simulation of Microsystems. 1998. pp.474-479.

[21] L.A Rocha, L. Mol, E. Cretu and R.F. Wolffenbuttel, Experimental verification of squeezed-film damping models for MEMS, In: MME'2005 (Micromechanics Europe), Gotenburg, Sweden, 4-6 Sept. 2005, pp. 244–247.

[22] PANDEY, A. K. – PRATAP, R.: A semi-analytical model for squeeze-film damping including rarefaction in a MEMS torsion mirror with complex geometry. Journ. of Micromechanics and Microengineering. 18 (2008) 105003. IOP Publishing Ltd, 2008. 12 pp.